fishes

MDPI

Article

Histological, Immunohistochemical, and Ultrastructural Characterization of Cartilage in Molly Fish (*Poecilia sphenops*): Insights into Skeletal Adaptations in Teleosts

Doaa M. Mokhtar [1,2], Mohammed A. Abdel-Ghani [3,*], Enas A. Abdelhafez [1], Marco Albano [4], Khalid M. Alkhodair [5] and Giacomo Zaccone [4,*]

[1] Department of Cell and Tissues, Faculty of Veterinary Medicine, Assuit University, Assiut 71526, Egypt; doaa@aun.edu.eg (D.M.M.); enas.mahmoud@vet.au.edu.eg (E.A.A.)
[2] Department of Histology and Anatomy, School of Veterinary Medicine, Badr University in Assiut, Assiut 71516, Egypt
[3] Department of Clinical Sciences, College of Veterinary Medicine, King Faisal University, Al-Ahsa 31982, Saudi Arabia
[4] Department of Veterinary Sciences, University of Messina, 98168 Messina, Italy; malbano@unime.it
[5] Department of Anatomy, College of Veterinary Medicine, King Faisal University, Al-Ahsa 31982, Saudi Arabia; kalkhodair@kfu.edu.sa
* Correspondence: mataha@kfu.edu.sa (M.A.A.-G.); zacconegiacomo@gmail.com (G.Z.)

Abstract: Cartilage is a crucial component of the vertebrate skeletal system, providing structural integrity, flexibility, and adaptive functions across species. In teleost fish, cartilage exhibits significant morphological and functional diversity, providing specialized biomechanical properties essential for aquatic life. This study presents a detailed histological, immunohistochemical, and ultrastructural investigation of cartilage in molly fish (*Poecilia sphenops*), identifying five distinct types of cartilage: hyaline-cell, scleral, cell-rich hyaline, elastic cell-rich, and matrix-rich hyaline cartilage. Histological staining techniques revealed notable differences in cellular architecture and composition of the extracellular matrix among the cartilage types. Immunohistochemical analysis demonstrated the expression of S100 protein and acetylcholinesterase (Ach), suggesting their involvement in cartilage regulation and maintenance. Endochondral ossification was observed in the head and gill arches. Electron microscopy provided detailed insights into chondrocyte morphology, interactions between cartilage and the perichondrium, and interactions between telocytes and fibroblasts. The findings enhance our understanding of skeletal adaptations in teleost fish, emphasizing the functional diversity of cartilage in aquatic environments. This study contributes to evolutionary biology and may have implications for regenerative medicine and biomaterials research.

Keywords: teleosts; skeletal adaptation; chondrocytes; perichondrium; osteogenesis

Key Contribution: This study presents a comprehensive characterization of cartilage types in *Poecilia sphenops*, revealing five structurally distinct forms with specialized functions. Histological and immunohistochemical analyses identified key proteins (S100, Ach) involved in cartilage regulation and mineralization. Endochondral ossification was documented in gill arches, indicating active skeletal maturation. Electron microscopy revealed chondrocyte structure and perichondrial interactions. Notably, telocytes were identified within the perichondrium, suggesting a role in cartilage maintenance and signaling. These findings provide new insights into skeletal adaptation in teleosts and offer potential implications for regenerative medicine.

Academic Editors: Stefanos Fragkoulis and Kevin J. Parsons

Received: 20 March 2025
Revised: 21 April 2025
Accepted: 28 April 2025
Published: 30 April 2025

Citation: Mokhtar, D.M.; Abdel-Ghani, M.A.; Abdelhafez, E.A.; Albano, M.; Alkhodair, K.M.; Zaccone, G. Histological, Immunohistochemical, and Ultrastructural Characterization of Cartilage in Molly Fish (*Poecilia sphenops*): Insights into Skeletal Adaptations in Teleosts. *Fishes* **2025**, *10*, 202. https://doi.org/10.3390/fishes10050202

1. Introduction

Cartilage is a crucial skeletal component in vertebrates, providing structural support and flexibility in various anatomical regions [1]. In teleost fish, cartilage exhibits a remarkable diversity of forms and functions, playing essential roles in both development and adaptation to aquatic environments [2]. Unlike cartilage in higher vertebrates, which primarily serves as a precursor to bone, fish cartilage can persist throughout life in specialized regions [3]. The unique composition and organization of cartilage in teleosts make it an intriguing subject for comparative histological and functional studies [4].

The structural and functional diversity of cartilage in teleosts suggest a high degree of evolutionary specialization [5]. Various types of cartilage play distinct roles in different anatomical locations, contributing to the mechanical properties, flexibility, and resilience required for life in aquatic environments [6].

Molly fish (*Poecilia sphenops*) are excellent models for studying cartilage because of their small size, ease of maintenance, and distinct skeletal features [7]. Previous research has identified multiple cartilage types in teleosts, each with unique cellular and extracellular matrix compositions [8,9].

Furthermore, cartilage plays an essential role in fish growth, regeneration, and biomechanical function [10]. Many species exhibit specialized adaptations in their cartilaginous tissues, allowing them to thrive in diverse aquatic environments [11,12]. Teleost fish exhibit a unique combination of chondrogenesis and osteogenesis [13], allowing researchers to explore the fundamental processes of skeletal formation, mineralization, and remodeling [14]. The ability of some fish species to regenerate cartilage suggests potential mechanisms that could be relevant for developing regenerative medicine approaches [15].

Understanding these processes can provide important evolutionary insights into cartilage development across vertebrates. While mammalian cartilage has been extensively studied, research on fish cartilage remains relatively limited. This study aims to expand our knowledge of cartilage biology by conducting detailed histological, immunohistochemical, and ultrastructural characterization of molly fish cartilage. The findings from this research will contribute to our understanding of skeletal adaptation in aquatic organisms and may offer potential applications in regenerative medicine and biomaterials.

2. Materials and Methods

2.1. Sample Collection

The study included 20 adult molly fish (*Poecilia sphenops*) that were randomly selected from a single commercial ornamental-fish supplier to minimize genetic and environmental variability. All fish were approximately of the same age (5–6 months) and had similar body weights (9.20 $\pm$ 1.20 g) and standard lengths (3.50 $\pm$ 0.4 cm), indicating comparable developmental stages. The fish were acclimated and maintained under standardized laboratory conditions (temperature: 26 $\pm$ 1 °C; photoperiod: 12 h light/12 h dark) for two weeks prior to sampling to ensure environmental uniformity. The sex of the fish was not determined, as the study's focus was not on sex-specific differences in cartilage structure. Prior to tissue sampling, all specimens were euthanized using an overdose of MS-222 (3% tricaine) in accordance with ethical standards [16].

2.2. Histological and Histochemical Analyses

Ten whole fish bodies were fixed immediately after death in Bouin's fluid for 22 h. Following ethanol dehydration and methyl benzoate clearance, the fixed tissues were embedded in paraffin wax. Harris hematoxylin and eosin, Crossmon's trichrome, oil red O, safranin-O, and a combination of PAS, AB, and HX were used to stain serial sagittal and transverse (5 μm thick) paraffin sections [17].

2.3. Histomorphometric Analysis

To quantify cartilage mineralization and chondrocyte distribution, histological images were analyzed using ImageJ software (v.1.54g). High-resolution sections stained with Alcian blue–PAS and H&E were captured at consistent magnification (scale bar = 50 μm). Fifteen representative images were selected for analysis based on visual evidence of distinct ossification stages. Mineralized regions were identified by color thresholding based on intensity and hue differences corresponding to cartilage-matrix mineralization. The mineralized-area ratio was calculated as the proportion of stained (darker) regions relative to the total tissue area in each image. Chondrocyte nuclei were detected by contrast-based contour identification using Gaussian blur and adaptive thresholding. Cell counts were performed on the entire field, and cell density was calculated as the number of cells per square millimeter (cells/mm^2), with pixel-to-micron conversion derived from the 50 μm scale bar (~110 pixels). All measurements were performed on uncompressed image files to ensure spatial accuracy.

2.4. Semithin Sections and TEM

Small gill arches of 10 specimens were preserved overnight in a 2.5% paraformaldehyde-glutaraldehyde solution. They were then osmicated with 1% osmium tetroxide in 0.1 Mol/L sodium-cacodylate buffer at pH 7.3 after washing in 0.1 Mol/L phosphate buffer. Following ethanol and propylene oxide dehydration, the specimens were embedded in Araldite. Semithin sections (1 μm thick) were stained with toluidine blue and viewed under a light microscope. Ultrotom-VRV (LKB Bromma, Stegen, Germany) was used to obtain ultrathin sections (70 nm), which were then stained with uranyl acetate and lead citrate. TEM images were obtained using a JEOL-100CX II electron microscope (Boston, MA, USA).

2.5. Immunohistochemical Analysis

For immunohistochemical investigation, sections of the head regions were prepared using the UltraTek HRP Anti-Polyvalent (DAB) Staining System (ScyTek Laboratories, West Logan, UT, USA, AMF080). Sections were cleaned with distilled water after being deparaffinized with xylene and rehydrated in graded ethanol. The sections were heated in a sodium citrate buffer (0.01 M, pH 6.0) for 10 min to increase epitope exposure. The slides were allowed to cool at room temperature for half an hour before they were cleaned with PBS. To reduce the endogenous peroxidase activity, the slides were immersed in distilled water containing 3% H_2O_2 for 15 min at room temperature. This step was followed by a PBS wash. The sections were blocked for five minutes at room temperature using the kit's blocking solution.

Primary antibodies against the S100 protein (Z0311, Dako, Glostrup, Denmark), rabbit polyclonal nicotinic acetylcholine R alpha 7 NACHRA7 (1:100; ABclonal, A7844, Wuhan, China), and mouse monoclonal ionized calcium-binding adaptor molecule (Iba-1, sc-32725, Santa Cruz Biotechnology, Heidelberg, Germany, diluted 1:200) were added to the sections, and the sections were then incubated for overnight at 4 °C. Simultaneously, tissue samples that were devoid of the S100 protein primary antibody and instead contained buffer were used as negative controls (Supplementary Figure S1). The secondary Ultra Tek HRP anti-polyvalent antibody (goat anti-mouse, -rabbit, and -guinea pig IgG), which was acquired from Scy Tek (El Paso, TX, USA), was incubated with the sections for 15 min after the sections had been rinsed three times for five minutes each with PBS. The slides were then cleaned for three minutes using a wash buffer, and the tissues were incubated with the HRP for fifteen minutes before being cleaned three times for three minutes each using a wash buffer. Diaminobenzodiazibin DAB chromogen diluted with DAB substrate (provided within the same Scy Tek Detection kit) was used to visualize the reaction according to the

manufacturer's protocol by staining 10–15 min until the desired staining was achieved; each section was then counterstained with Harris hematoxylin and mounted with DPX.

2.6. Antibody Specificity

Nicotinic and muscarinic receptors of acetylcholine are widely expressed in the CNS and in non-neural tissues such as epithelia, macrophages, and keratinocytes. Based on earlier morphological and PCR analyses conducted in zebrafish and other teleost fish species, the NACHRA7 was targeted in this investigation [18–20].

3. Results

3.1. Histological Analysis

Hyaline-cell, scleral, elastic-cell rich, cell-rich hyaline, and matrix-rich hyaline cartilage are the five primary forms of cartilage. The most prevalent type of cartilage is the hyaline-cell type.

In molly fish, hyaline-cell cartilage (HCC) is dispersed throughout the head. It is distributed in the core of the nasal skin flaps and in the olfactory region, lips, rostral folds, barbels, and pre-palatine and submaxillary menisci and next to the facial nerve. In addition, HCC is found in the pectoral girdle, gill arches, and ligaments (Figure 1A,B).

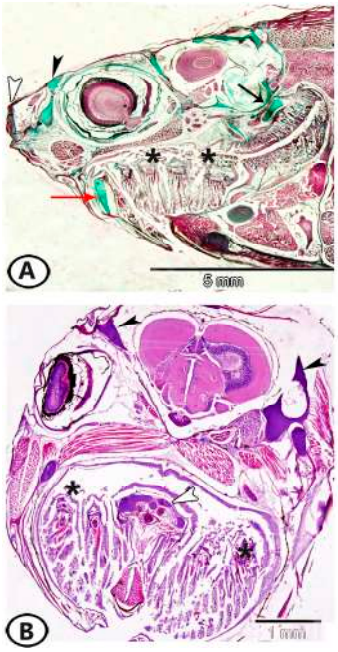

Figure 1. Distribution of hyaline-cell cartilage (HCC) in the head region of molly fish. (**A**) A sagittal section of the head region showing that HCC is distributed in the core of the nasal skin flaps and in the olfactory region (black arrowhead), lips, rostral folds (white arrowhead), and pre-palatine and submaxillary menisci (red arrow). In addition, it occurs in the pectoral girdle (black arrow) and gill arches (asterisks). (**B**) A transverse section of the head region of molly fish showing distribution of HCC in the head (black arrowheads), gill arches (asterisks), and ligaments (white arrowhead).

The HCC consists of densely packed cells with minimal extracellular matrix, which contains collagen fibers (Figure 2A). HCC cells can be arranged in distinct row patterns (Figure 2B). Two subtypes of HCC have been identified: fibrohyaline-cell cartilage (chondroid cartilage) (Figure 2C), which is characterized by a matrix rich in prominent collagen fibers, and lipohyaline-cell cartilage (Figure 2D), a rare variant that contains a mixture of hyaline and fat cells.

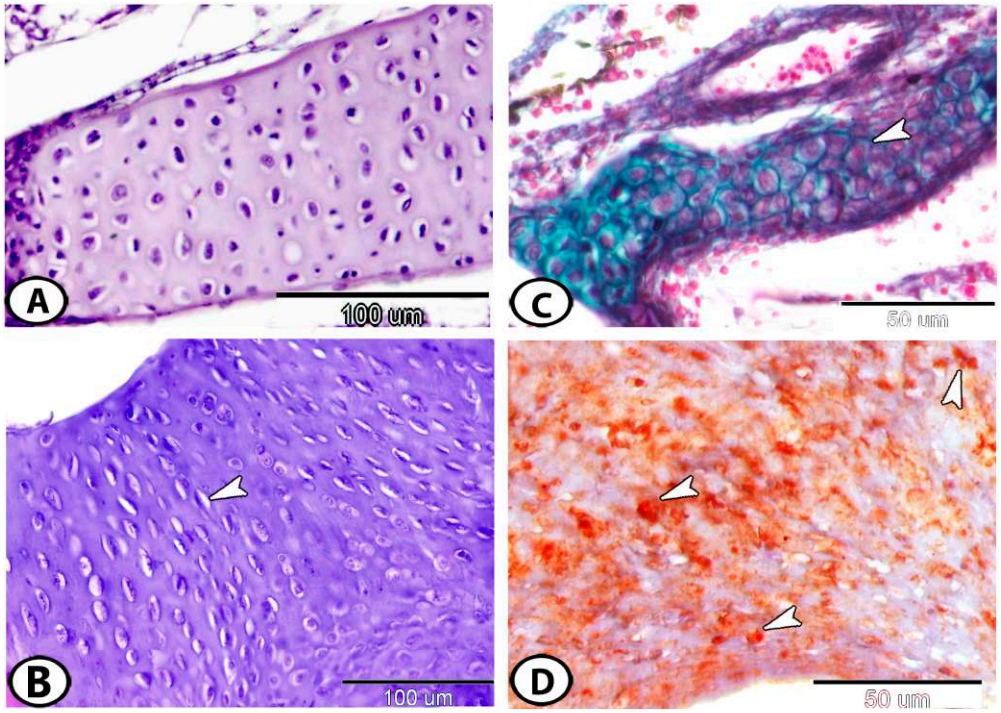

Figure 2. (**A**) The gill arch of molly fish has hyaline cell cartilage that is similar to that of mammals (HE). (**B**) Around the olfactory region, hyaline cartilage cells are grouped in rows (arrowhead) (HE). (**C**) Fibro-hyaline cell cartilage (arrowhead) in the gill arch (Crossmon's trichrome). (**D**) A transverse section of lipohyaline cell cartilage showing lipid droplets (arrowheads) in the lower jaw (Oil red O).

The matrix's sulfated glycosaminoglycans are stained with safranin O (Figure 3A) and alcian blue (Figure 3B). HCC is typically connected to the articular surface by collagenous fibers (Figure 3B) or is found in association with skeletal muscle fibers (Figure 3C). The scleral cartilage forms a protective plate around the outer part of the eye and consists of one or two rows of closely packed cells (Figure 3D).

A form of hyaline cartilage known as cell-rich hyaline cartilage (CRHC) has cells or lacunae that make up over half of the tissue volume. It commonly forms epiphyseal cartilages (Figure 4A). Elastic cell-rich cartilage (ECRC) (Figure 4B) is a highly cellular cartilage that has an elastic, fiber-rich matrix. It is frequently found in gill filaments and lips, where a thick, fibrous perichondrium envelops it.

Matrix-rich hyaline cartilage (MRHC) represents the typical form of hyaline cartilage. The chondrocytes appear shrunken within lacunae and are separated by a substantial amount of extracellular matrix. MRHC is commonly found in the gill arches and periosteal pad (Figure 4C,D).

Endochondral ossification is the process by which bone replaces cartilage. In the gill arch, mesenchymal cells aggregate and differentiate into chondrocytes, forming a cartilage model of future bone (Figure 5A,B). Within this model, chondrocytes proliferate (Figure 5C), then enlarge (hypertrophy), modifying the extracellular matrix. The cartilage matrix becomes partially mineralized (Figure 5D). Chondrocytes in the hypertrophic zone undergo apoptosis, leaving behind a network of calcified cartilage. The blood vessels then invade the calcified cartilage to deliver osteoblasts that contribute to bone formation. The initial woven bone is remodeled into lamellar bone (Figure 5E). In the gill arch, a central cartilaginous zone containing well-defined cell clusters is surrounded by a layer of acellular mineralized bone (Figure 5F). To enhance the qualitative observations of endochondral ossification, quantitative histomorphometric analysis was conducted. The mineralized area comprised approximately 78% of the total tissue area, with a chondrocyte density of 715.94 cells/mm^2.

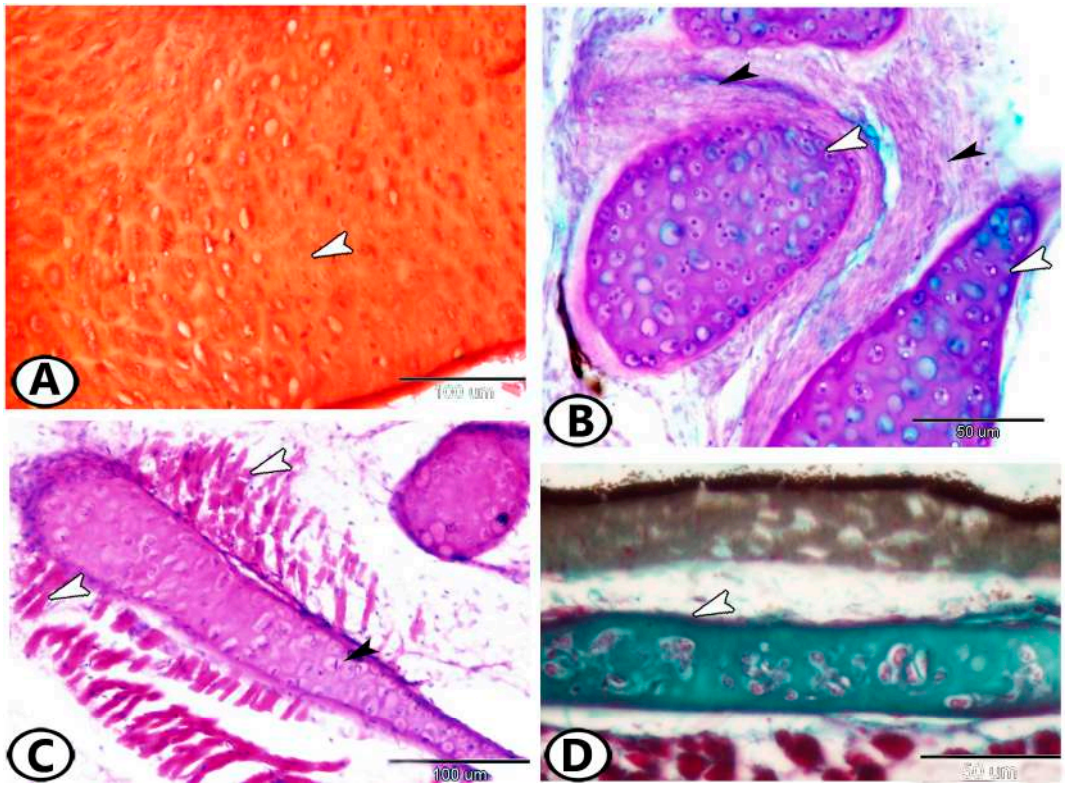

Figure 3. (**A**) The cartilage around the inner ear shows safranin-positive matrix (arrowhead). (**B**) HCC (white arrowheads) attached to collagenous fibers (black arrowheads) in the dorsal fin (AB/PAS/HX). (**C**) HCC (black arrowhead) attached to skeletal muscle fibers (white arrowheads) in the buccal cavity (HE). (**D**) Scleral cartilage (arrowhead) (Crossmon's trichrome).

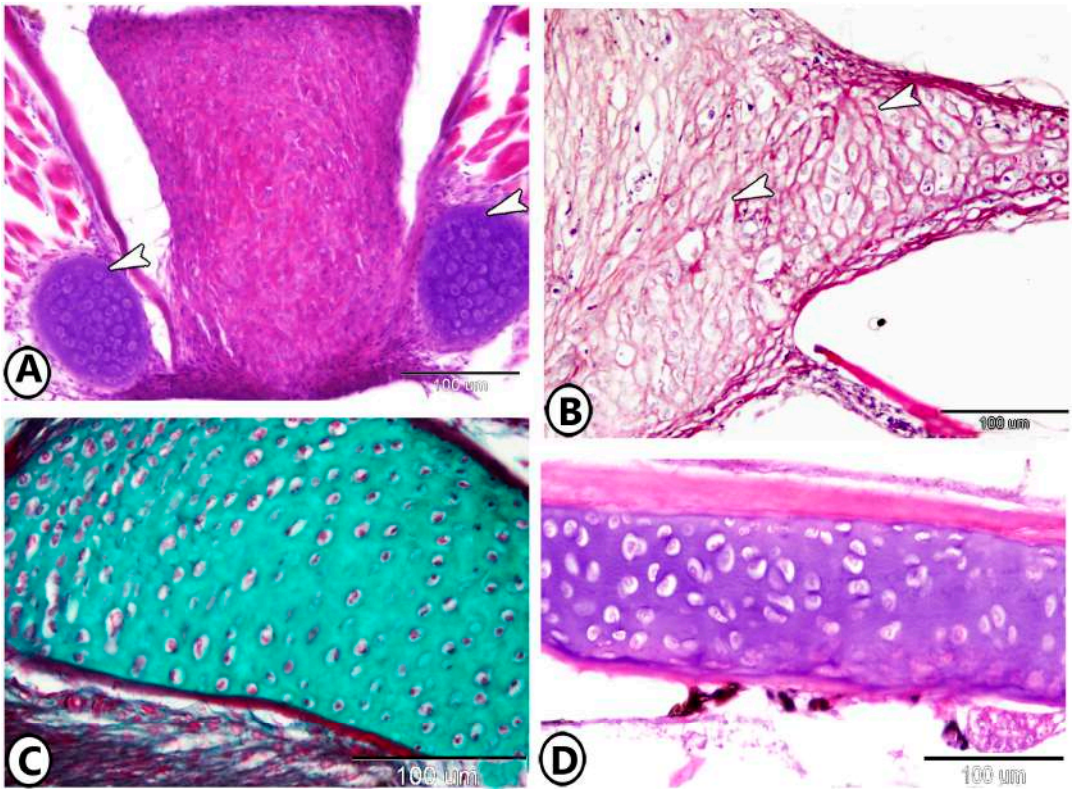

Figure 4. (**A**) CRHC (arrowheads) in the epiphysis of the tongue (HE). (**B**) Elastic/cell-rich cartilage (arrowhead) in the lower lip (HE). (**C**,**D**) MRHC in the periosteal pad and gill arch, respectively (Crossmon's trichrome and HE, respectively).

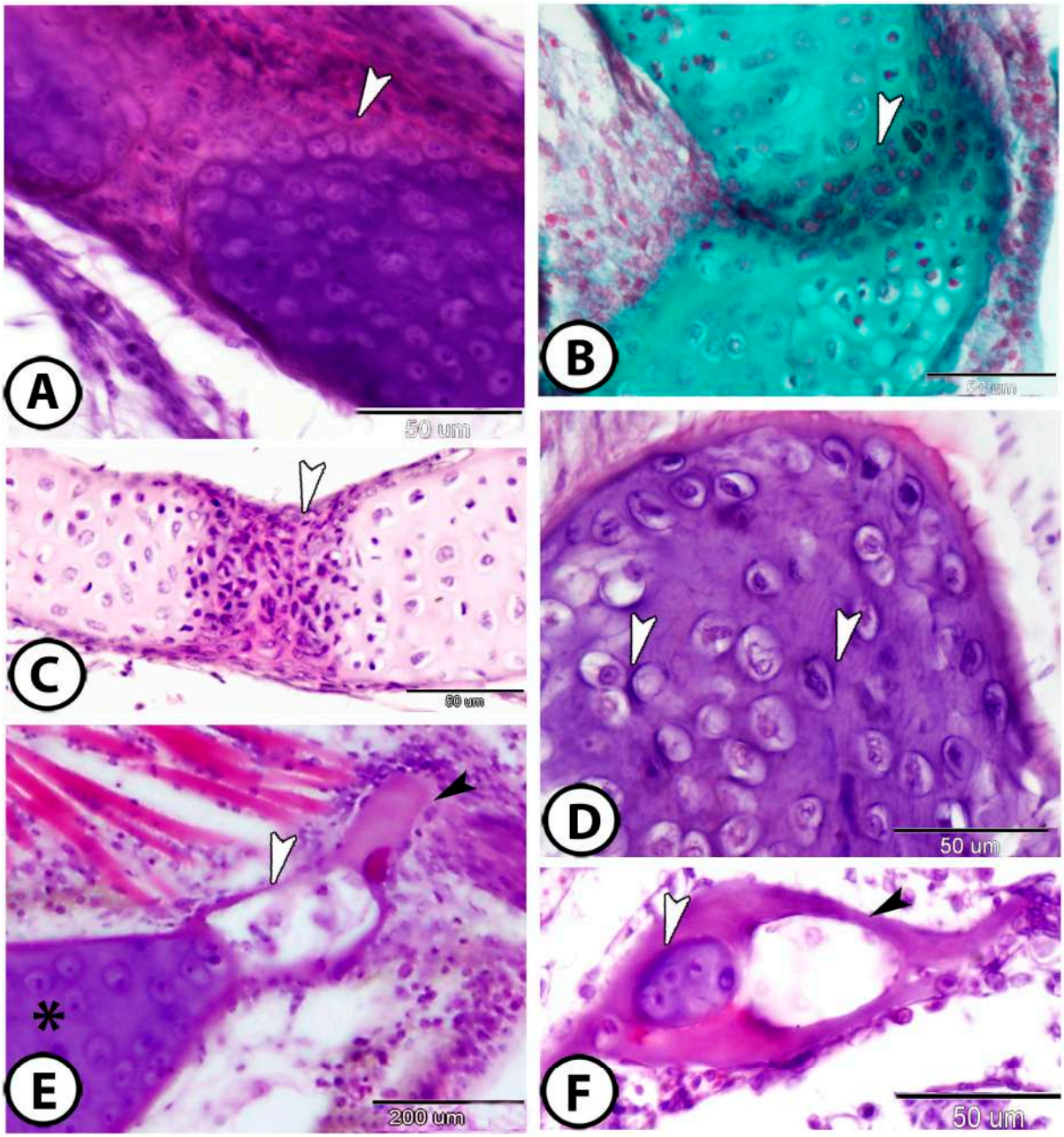

Figure 5. Endochondral ossification. (**A**,**B**) Mesenchymal cells (arrowheads) invade the cartilage in the gill arch (HE, Crossmon's trichrome, respectively). (**C**) The chondrocytes in the growth plate increased in number (arrowhead) (HE). (**D**) In the otic region of the neurocranium, the large chondrocytes in the calcified cartilage were dispersed throughout the cartilage in lacunae that were separated from the deeply basophilic extracellular matrix (arrowhead) (HE). (**E**) The blood vessels (white arrowhead) invade the cartilage (asterisk), facilitating bone formation by delivering osteogenic cells; newly forming bone is indicated by the black arrowhead. (**F**) A central cartilaginous zone (white arrowhead) is encircled by a layer of acellular mineralized bone (black arrowhead) (HE).

Semithin sections revealed that the cells forming the gill arch were arranged in an organized manner and positioned closely together (Figure 6A,B). In the primary gill lamellae, the chondrocytes formed a segmented arrangement (Figure 6C). Large, elongated chondrocytes were enclosed within lacunae and surrounded by a deeply stained perichondrium (Figure 6D). The chondrocytes displayed vacuolated cytoplasms and deeply stained nuclei, and the matrix exhibited a metachromatic reaction to toluidine blue (Figure 6E). Additionally, the cartilage was surrounded by numerous interstitial cells (Figure 6F).

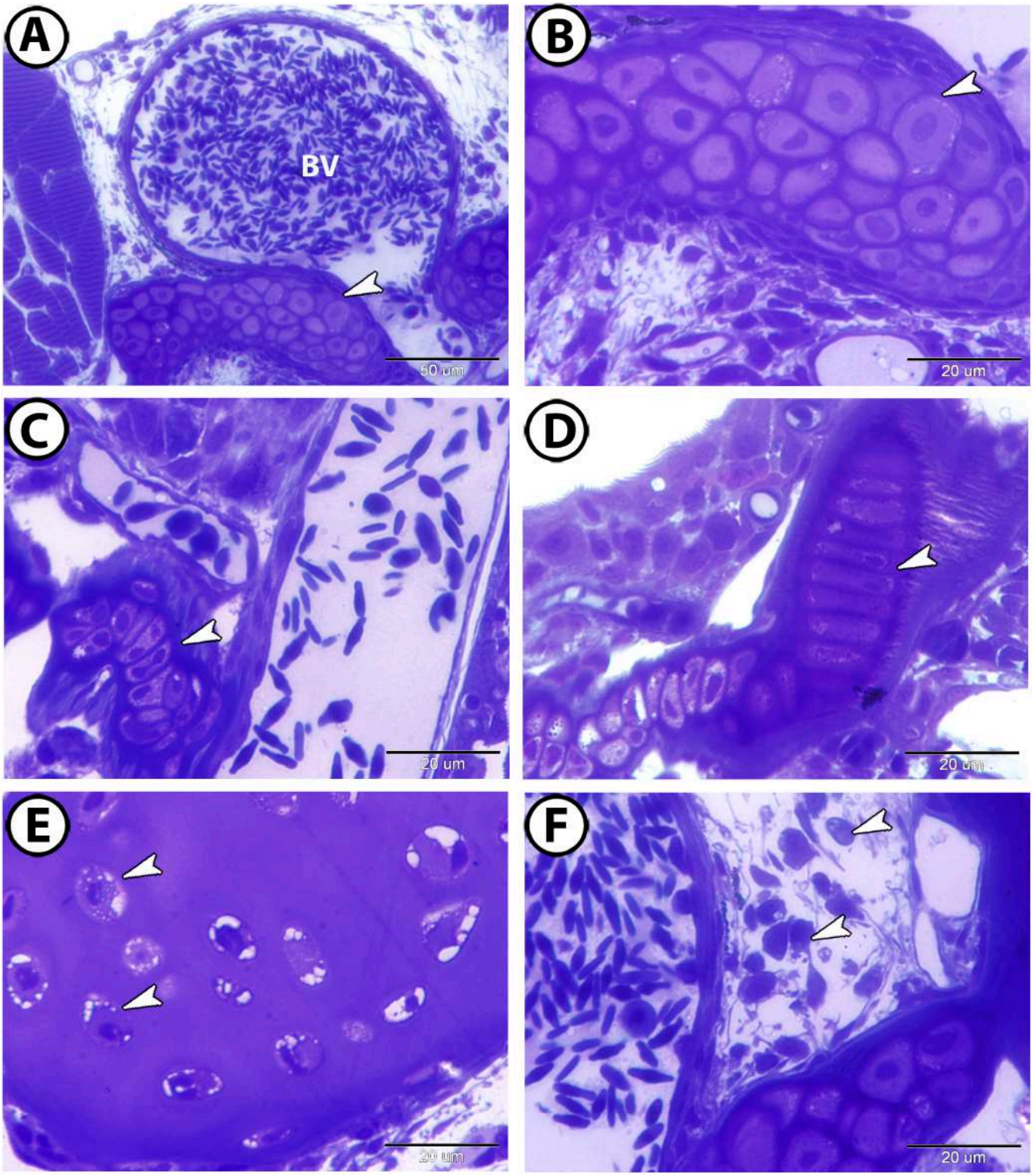

Figure 6. Semithin sections of the cartilage in the gill arch, stained with toluidine blue. (**A**,**B**) The chondrocytes are arranged in an organized manner and in close proximity to one another (arrowheads). Note the presence of large blood vessels (BV). (**C**) The chondrocytes are arranged in a segmented appearance in the primary gill lamellae (arrowhead). (**D**) Large, elongated chondrocytes enclosed in lacunae and surrounded by deeply stained perichondrium (arrowhead). (**E**) The chondrocytes exhibit vacuolated cytoplasm and deeply stained nuclei (arrowheads). (**F**) The cartilage is surrounded by many interstitial cells (arrowheads).

3.2. Immunohistochemistry

S100 protein was expressed in both the extracellular matrix (Figure 7A) and chondrocytes of the gill arch (Figure 7B). Acetylcholinesterase (Ach) was detected on the cell surfaces of chondrocytes in the mouth cavity (Figure 7C,D). The processes of endochondral ossification and cartilage-to-bone transformation were observed through staining for Iba1, which was specifically expressed in hypertrophic and calcified cartilage (Figure 8).

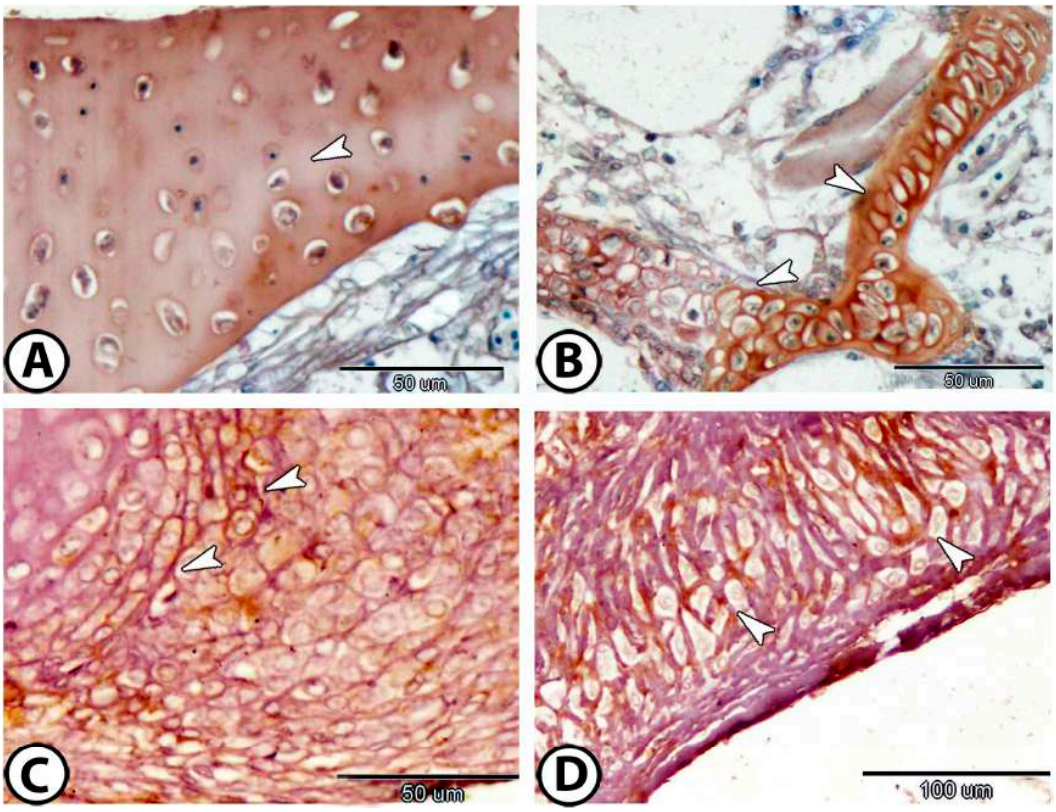

Figure 7. Immunohistochemistry. (**A**,**B**) S100Protein expression in the matrix and chondrocytes, respectively (arrowheads). (**C**,**D**) Ach expression on the cell surfaces of chondrocytes (arrowheads).

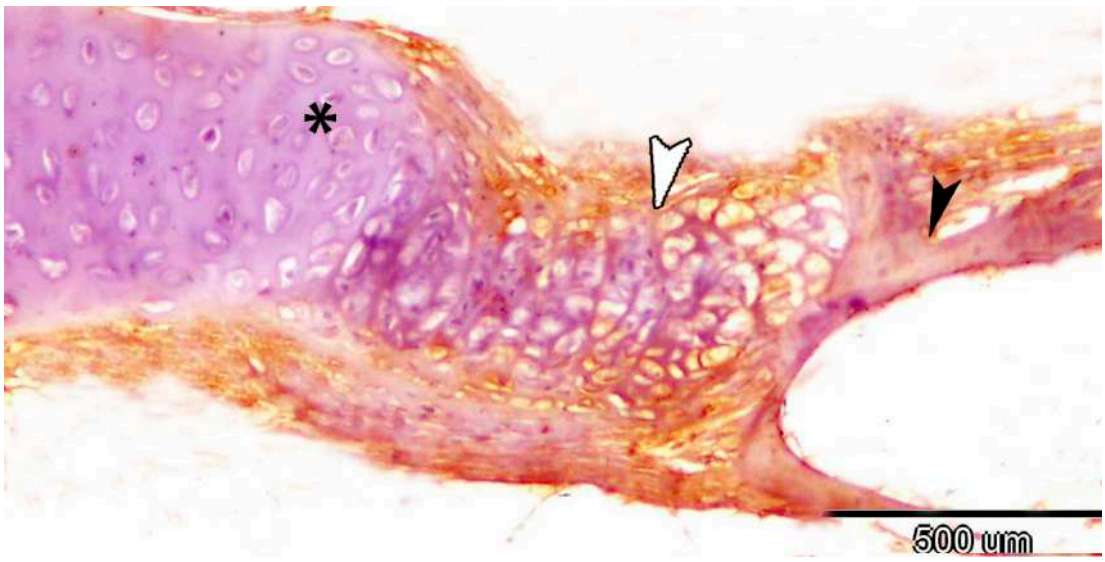

Figure 8. Immunohistochemistry of iba1 showing the processes of endochondral ossification (white arrowhead) and transformation of cartilage (asterisk) to bone (black arrowhead).

3.3. Electron Microscopy

The cartilage of the gill arch predominantly consists of hyaline-cell cartilage, the most abundant and representative type in *Poecilia sphenops*. The perichondrium consists of cellular layers of fibroblasts and chondroblasts. The chondroblasts appeared as fusiform cells with multiple cell processes and heterochromatic nuclei (Figure 9A,B). Their cytoplasms contained mitochondria and rough endoplasmic reticulum (rER) (Figure 9C,D).

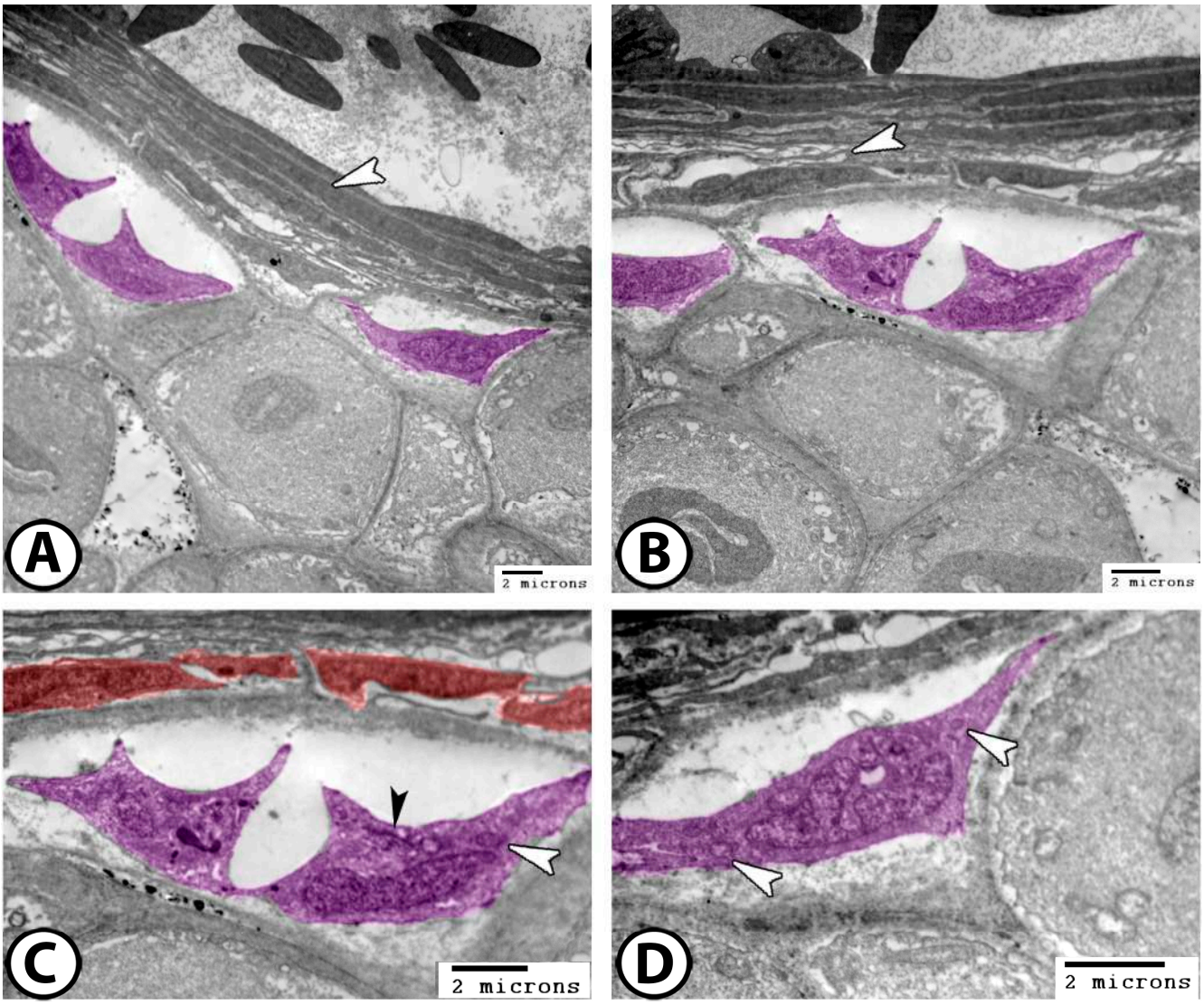

Figure 9. Digitally colorized TEM images of the cartilages of the gill arch. (**A**,**B**) The perichondrium consists of fibroblasts (arrowheads) and chondroblasts (violet). (**C**,**D**) The chondroblasts (violet) contain mitochondria (white arrowheads) and rER (black arrowhead). Note the presence of fibroblasts (red).

The cytoplasms of chondrocytes contain mitochondria, lipids, rER, ribosomes, and micropinocytotic vesicles (Figure 10A,B). The perichondrium is surrounded by numerous interstitial cells, with telocytes (TCs) being the most dominant. The TCs observed here featured fusiform cell bodies and multiple long processes known as telopodes (Tps) (Figure 10C,D). These TCs extended their Tps around interstitial immune cells (Figure 10C) and established heterocellular contacts with fibroblasts (Figure 10D).

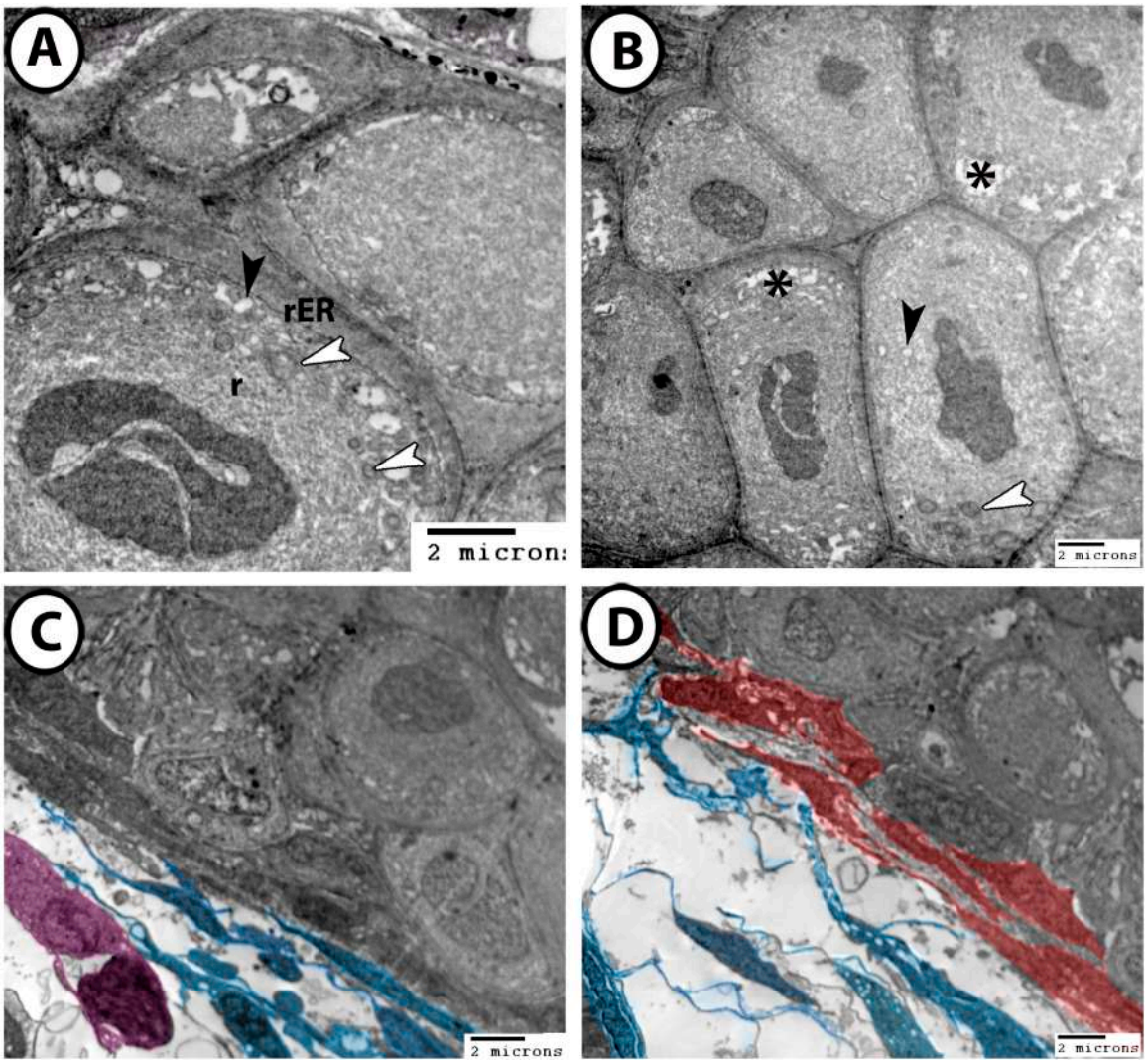

Figure 10. Digitally colorized TEM images of the cartilages of the gill arch. (**A**,**B**) The chondrocytes contained mitochondria (white arrowheads), lipids (asterisks), rER, ribosomes (r), and micropinocytotic vesicles (black arrowheads). (**C**) TCs and their Tps (blue) made direct contact with interstitial immune cells (violet). (**D**) TCs and Tps (blue) established heterocellular contacts with fibroblasts (red).

4. Discussion

The diversity of cartilaginous structures among fish species underscores the functional significance of cartilaginous tissue in aquatic adaptation. While molly fish express five distinct cartilage types, other teleosts like *Ctenopharyngodon idella* and *Sphaerichthys osphromenoides* express an additional cartilage type in the submaxillary meniscus called fibro/cell-rich cartilage, which is characterized by a high density of collagen fibers in the cartilage matrix [6,21]. The presence of five distinct cartilage types in molly fish highlights the complexity and specialization of cartilaginous structures in teleost fish. These findings support those of previous studies on cartilage differentiation in vertebrates [6,9]. For example, zebrafish and medaka exhibit variations in chondrocyte organization and matrix composition that may influence skeletal flexibility and growth dynamics [2]. In sturgeons and paddlefish, cartilage plays a crucial role in their elongated rostra and sensory functions. The rostral cartilage supports electroreceptors that enable the fish to detect prey in murky waters [22]. Unlike teleosts, sturgeons maintain a significant portion of their endoskeleton as cartilage throughout life, representing an intermediate evolutionary stage between cartilaginous and bony fishes [23].

HCC was identified as the most abundant cartilage type, particularly in the head region, where it provides structural support for sensory and feeding structures [8]. The two subtypes, fibrohyaline-cell cartilage and lipohyaline-cell cartilage, demonstrate functional diversity, with the former being more fibrous and the latter incorporating lipid-rich elements. This differentiation may be crucial for biomechanical properties required at different anatomical locations. Similar findings in red-tail sharks and Orinoco sailfin catfish suggest phylogenetic adaptation to species with specialized feeding behaviors [6].

The identification of the scleral cartilage forming a protective plate around the eye is consistent with previous descriptions of fish ocular anatomy [24]. This cartilage type likely plays a crucial role in maintaining ocular integrity and function, particularly in aquatic environments, where mechanical protection is essential [25].

CRHC is predominantly observed in epiphyseal cartilage, where it contributes to growth and skeletal remodeling. The high cellular density suggests active chondrogenesis, a key process in skeletal development. This hypothesis is further supported by the observed osteogenic transformation, in which calcified cell-rich hyaline cartilage transitions into bone. The osteogenic process identified in the gill arch, with mesenchymal cell invasion and the formation of mineralized bone layers, is consistent with the endochondral ossification patterns reported in other teleosts [26,27].

Ossification of cartilage can occur in adult fish, but its extent and mechanism depend on the species and skeletal region. In many teleost fish, cartilage serves as a precursor to bone through endochondral ossification, a process by which bone progressively replaces cartilage [28]. This process is particularly evident in growth plates, vertebrae, and fins [29]. In adult fish, remodeling and mineralization can continue based on growth demands and environmental factors. The development of the jaw of the male Atlantic salmon (*Salmo salar*) during their spawning run depends particularly on this capacity [30]. However, in some adult fish, particularly in species that rely on flexible cartilage for feeding or locomotion (e.g., sharks and rays), certain cartilaginous structures remain unossified throughout life [31]. In contrast, teleosts exhibit continuous remodeling and ossification in specific regions, such as the skull and gill arches, where mineralized bone progressively replaces cartilage [32]. In species with continued growth, like zebrafish, epiphyseal plates (growth zones) remain active, allowing longitudinal bone growth [33].

Research on sea bream (*Sparus aurata*), a marine teleost, has characterized the cellular organization and modifications accompanying endochondral and dermal bone formation during skeletal ontogeny, providing insights into the diversity of ossification processes among teleost fish [4]. Studies on fish skeletal development have also identified calcified cartilage, an intermediate stage in which cartilage becomes mineralized but does not fully transition into bone. This is commonly observed in structures such as gill arches and jaw elements, where partial ossification provides both rigidity and flexibility [34].

Comparative studies have shown that genes such as *Sox9* and *Col2a1* play fundamental roles in cartilage formation and differentiation across vertebrates [35]. *Sox9* acts as a master transcription factor that initiates chondrogenesis, while *Col2a1* encodes type II collagen, a key structural component of the cartilage extracellular matrix [36]. In both chondrichthyans and teleosts, these genes exhibit conserved expression patterns during early cartilage development [37]. In zebrafish, *Sox9a* and *Sox9b* are expressed in craniofacial cartilage and fin endoskeletons, while *Col2a1a* is expressed in notochordal and cranial cartilaginous structures [38]. Similarly, in cartilaginous fish such as the catshark (*Scyliorhinus canicula*), *Sox9* and *Col2a1* are expressed throughout the hyaline cartilage-rich endoskeleton [39]. The observed cartilage diversity in *Poecilia sphenops*, including the presence of matrix-rich and cell-rich cartilage subtypes, suggests differential regulation of these conserved molecular pathways, potentially reflecting adaptive modulation during teleost evolution. Future

work incorporating in situ hybridization or transcriptomic profiling of *Sox9* and *Col2a1* in *Poecilia sphenops* could clarify the molecular mechanisms underlying cartilage subtype specification and its evolutionary significance.

The present study identified the expression of s100 protein, acetylcholinesterase, and iba1 in fish cartilage for the first time. Immunohistochemical analysis revealed significant expression of S100 protein in chondrocytes and the matrix, a finding that aligns with its known role in calcium binding and cartilage mineralization [40,41]. Additionally, acetylcholinesterase (Ach) expression in chondrocyte surfaces suggests a possible regulatory role in cartilage function, as previously indicated in osteoarthritis studies [42]. These findings indicate that non-neuronal cholinergic signaling may be involved in maintenance and remodeling of fish cartilage, a topic that warrants further investigation. The expression of Iba1 in endochondral ossified cartilage suggests that macrophages and osteoclast-like cells play an active role in bone formation, cartilage resorption, and remodeling [43,44]. This highlights the interplay between the immune system and skeletal development, reinforcing the notion that macrophages are essential for proper bone homeostasis [45]. Furthermore, the extraction from fish cartilage of glycosaminoglycans such as chondroitin sulfate, dermatan sulfate, and hyaluronic acid has been the subject of numerous investigations [46,47].

Ultrastructural examination of *Poecilia sphenops* cartilage revealed a highly organized cellular and extracellular architecture that reflects the functional complexity of teleost skeletal tissues. Chondrocytes were enclosed within well-defined lacunae and exhibited prominent organelles such as rough endoplasmic reticulum, mitochondria, ribosomes, and micropinocytotic vesicles, features indicative of active matrix synthesis and metabolic function [48]. The perichondrium was composed of fibroblasts and chondroblasts, with the latter displaying elongated profiles and dense cytoplasm, suggesting a role in cartilage maintenance and renewal [49]. These ultrastructural features are consistent with those reported in other advanced teleosts such as zebrafish [3] and the cichlid *Hemichromis bimaculatus* [5], which also exhibit diverse cartilage phenotypes adapted for biomechanical efficiency. In contrast, the cartilage of more basal vertebrates, such as lampreys or cartilaginous fish, tends to show less cellular specialization and less complexity in the extracellular matrix [50]. These findings emphasize the evolutionary advancement of teleost cartilage, which is marked by increased cellular diversity and regulatory interactions that support structural adaptation and tissue homeostasis.

The identification of telocytes (TCs) within the perichondrium of *Poecilia sphenops* adds a novel dimension to our understanding of cartilage regulation in teleosts. Telocytes are interstitial cells characterized by a small cell body and extremely long, slender projections known as telopodes, which establish close contacts with immune cells and blood vessels [51]. In the present study, TCs extended their telopodes to the interstitial fibroblasts and immune cells, suggesting a potential role in local signaling and tissue coordination. Similar observations have been reported in other vertebrate tissues, including the intestines of rainbow trout (*Oncorhynchus mykiss*) [52], the cardiac stomach of Nile catfish (*Clarias gariepinus*) [53], the heart of molly fish (*Poecilia sphenops)* [54], and the pancreas of reptiles [55], where telocytes are implicated in tissue remodeling, regeneration, and immune modulation. Their presence within the perichondrium of *P. sphenops* cartilage may indicate involvement in cartilage homeostasis, possibly through mediating interactions between chondroblasts, immune cells, and extracellular matrix components. These findings support emerging hypotheses that telocytes participate in tissue repair and signaling across diverse organ systems [56] and extend their relevance to skeletal tissues in teleost fish. Further molecular characterization, such as CD34 or PDGFRα immunolabeling, could help clarify their functional roles in cartilage biology.

5. Conclusions

This study provides a comprehensive characterization of cartilage in *Poecilia sphenops*, revealing five morphologically distinct types with specialized structural and cellular features. Through a combination of histological, immunohistochemical, and ultrastructural analyses, we demonstrated the complex organization of chondrocytes, matrix composition, and perichondrial components across different cartilage types. Additionally, the observed endochondral ossification in gill arches and cranial regions contributes to our understanding of skeletal development in fish. The expression of S100 and acetylcholinesterase proteins highlights potential regulatory mechanisms involved in cartilage maintenance and signaling. The presence of telocytes within the perichondrium further suggests a novel role for these cells in cartilage maintenance and tissue remodeling, which could have implications for future biomedical applications. In particular, recent evidence points to a function of fish telocytes in the regulation of multiple processes, including homeostasis, tissue regeneration, and immunosurveillance. Together, these findings contribute to a deeper understanding of teleost cartilage diversity. Future research integrating molecular and genetic analyses will be essential for uncovering the mechanisms governing cartilage differentiation and adaptation in aquatic vertebrates.

Supplementary Materials: The following supporting information can be downloaded at: https://www.mdpi.com/article/10.3390/fishes10050202/s1, Figure S1: Negative control in which S100 protein is omitted and replaced by buffer.

Author Contributions: Study design, methodology, interpretation, manuscript preparation, manuscript revision: D.M.M., E.A.A., M.A. and M.A.A.-G.; study supervision, methodology, writing—review and editing, K.M.A. and G.Z. All authors have read and agreed to the published version of the manuscript.

Funding: This work was supported through the Annual Funding track by the Deanship of Scientific Research, Vice Presidency for Graduate Studies and Scientific Research, King Faisal University, Saudi Arabia [Project No. KFU251653].

Institutional Review Board Statement: The current work was carried out in compliance with university animal care rules and Egyptian laws. Every procedure used in this study has been authorized by the National Ethical Committee of the Faculty of Veterinary Medicine at Assiut University in Egypt. The Ethical No. is Aun/vet/4/0015.

Informed Consent Statement: Not applicable.

Data Availability Statement: The data that support the findings of this study are available on request from the corresponding author.

Conflicts of Interest: We declare that there is no conflict of interest that could be perceived as prejudicing the impartiality of the research reported.

References

1. Fox, S.A.J.; Bedi, A.; Rodeo, S.A. The basic science of articular cartilage: Structure, composition, and function. *Sports Health* **2009**, *1*, 461–468. [CrossRef]
2. Witten, P.E.; Huysseune, A.; Hall, B.K. A practical approach for the identification of the many cartilaginous tissues in teleost fish. *J. Appl. Ichth.* **2010**, *26*, 257–262. [CrossRef]
3. Dewit, J.; Witten, P.E.; Huysseune, A. The mechanism of cartilage subdivision in the reorganization of the zebrafish pectoral fin endoskeleton. *J. Exp. Zool.* **2011**, *316B*, 584–597. [CrossRef]
4. Estêvão, M.D.; Silva, N.; Redruello, B.; Costa, R.; Gregório, S.; Canário, A.V.; Power, D.M. Cellular morphology and markers of cartilage and bone in the marine teleost *Sparus auratus*. *Cell Tissue Res.* **2011**, *343*, 619–635. [CrossRef]
5. Huysseune, A.; Sire, J.Y. Development of cartilage and bone tissues of the anterior part of the mandible in cichlid fish: A light and TEM study. *Anat. Rec.* **1992**, *233*, 357–375. [CrossRef] [PubMed]

6. Mokhtar, D.M. The skeleton of fish. In *Fish Histology: From Cells to Organs*, 2nd ed.; Mokhtar, D.M., Ed.; Apple Academic Press: New York, NY, USA, 2007; Volume 3, pp. 154–196. [CrossRef]
7. Alda, F.; Reina, R.G.; Doadrio, I.; Bermingham, E. Phylogeny and biogeography of the *Poecilia sphenops* species complex (*Actinopterygii*, *Poeciliidae*) in Central America. *Mol. Phyl. Evol.* **2013**, *66*, 1011–1026. [CrossRef] [PubMed]
8. Benjamin, M. Hyaline-cell cartilage (chondroid) in the heads of teleosts. *Anat. Embryol.* **1989**, *179*, 285–303. [CrossRef]
9. Benjamin, M.; Ralphs, J.R.; Eberewariye, O.S. Cartilage and related tissues in the trunk and fins of teleosts. *J. Anat.* **1992**, *181*, 113–118. [PubMed Central]
10. Zamani, A.; Khajavi, M.; Nazarpak, M.H.; Solouk, A.; Atef, M. Preliminary evaluation of fish cartilage as a promising biomaterial in cartilage tissue engineering. *Ann. Anat.* **2024**, *253*, 152232. [CrossRef]
11. Chaumel, J.; Schotte, M.; Bizzarro, J.J.; Zaslansky, P.; Fratzl, P.; Baum, D.; Dean, M.N. Co-aligned chondrocytes: Zonal morphological variation and structured arrangement of cell lacunae in tessellated cartilage. *Bone* **2020**, *134*, 115264. [CrossRef]
12. Zylberberg, L.; Meunier, F.J. New data on the structure and the chondrocyte populations of the haemal cartilage of abdominal vertebrae in the adult carp *Cyprinus carpio* (*Ostariophysii*, *Cyprinidae*). *Cybium* **2008**, *32*, 225–239. [CrossRef]
13. Witten, P.E.; Huysseune, A. Mechanisms of chondrogenesis and osteogenesis in fins. In *Fins and Limbs: Evolution, Development, and Transformation*; Witten, P.E., Huysseune, A., Eds.; The University of Chicago Press: Chicago, IL, USA, 2006; pp. 79–92. Available online: https://biblio.ugent.be/publication/8646018 (accessed on 20 March 2024).
14. Witten, P.E.; Huysseune, A.A. comparative view on mechanisms and functions of skeletal remodelling in teleost fish, with special emphasis on osteoclasts and their function. *Biol. Rev. Camb. Philos. Soc.* **2009**, *84*, 315–346. [CrossRef] [PubMed]
15. Ríos-Flores, A.J.; López-Flores, S.; Martínez-Moreno, J.A.; Falcon-Romero, K.Y.; Asencio-Alcudia, G.G.; Sepúlveda-Quiroz, C.A.; Martínez-García, R.; Rodríguez-Salazar, E.; González, C.A.A.; Maldonado, E. Regeneration of the caudal fin of the evolutionary ancient tropical gar *Atractosteus tropicus*. *BMC Zool.* **2024**, *9*, 26. [CrossRef]
16. Posner, L.P.; Scott, G.N.; Law, J.M. Repeated exposure of goldfish (*Carassius auratus*) to tricaine methanesulfonate (MS-222). *Zo. Wild. Med.* **2013**, *44*, 340–347. [CrossRef] [PubMed]
17. Bancroft, F.J.; Gamble, M. *Theory and Practice of Histological Techniques*, 6th ed.; Bancroft, J.D., Gamble, M., Eds.; Churchill Livingstone Elsevier: Philadelphia, PA, USA, 2008; Volume 172, pp. 593–620. [CrossRef]
18. Ackerman, K.M.; Boyd, R.T. Analysis of nicotinic acetylcholine receptor (nAChR) gene expression in zebrafish (*Danio rerio*) by in situ hybridization and PCR. In *Nicotinic Acetylcholine Receptor Technologies Neuromethods*; Ackerman, K.M., Boydvol, R.T., Eds.; Springer: New York, NY, USA, 2016; pp. 1–31. [CrossRef]
19. Capillo, G.; Zaccone, G.; Cupello, C.; Fernandes, J.M.O.; Viswanath, K.; Kuciel, M.; Zuwala, K.; Guerrera, M.C.; Aragona, M.; Icardo, J.M. Expression of acetylcholine, its contribution to regulation of immune function and O_2 sensing and phylogenetic interpretations of the African Butterfly Fish *Pantodon buchholzi* (Osteoglossiformes, Pantodontidae). *Fish Shellfish Immunol.* **2021**, *111*, 189–200. [CrossRef] [PubMed]
20. Zaccone, G.; Alesci, A.; Mokhtar, D.M.; Aragona, M.; Guerrera, M.C.; Capillo, G.; Albano, M.; de Oliveira Fernandes, J.; Kiron, V.; Sayed, R.K.A.; et al. Localization of acetylcholine, alpha 7-nachr and the antimicrobial peptide piscidin 1 in the macrophages of fish gut: Evidence for a cholinergic system, diverse macrophage populations and polarization of immune responses. *Fishes* **2023**, *8*, 43. [CrossRef]
21. Benjamin, M. The cranial cartilages of teleosts and their classification. *J. Anat.* **1990**, *169*, 153–172. [PubMed] [PubMed Central]
22. Grande, L.; Bemis, W.E. Osteology and phylogenetic relationships of fossil and recent Paddlefishes (Polyodontidae) with comments on the interrelationships of Acipenseriformes. *J. Vert. Paleon.* **1991**, *11*, 1–121. [CrossRef]
23. Bemis, W.E.; Findeis, E.K.; Grande, L. An overview of Acipenseriformes. *Env. Biol. Fish.* **1997**, *48*, 25–71. [CrossRef]
24. Faustino, M.; Power, D.M. Osteologic development of the viscerocranial skeleton in sea bream: Alternative ossification strategies in teleost fish. *J. Fish. Biol.* **2005**, *58*, 537–572. [CrossRef]
25. Franz-Odendaal, T.A. The elusive scleral cartilages: Comparative anatomy and development in teleosts and avians. *Anat. Rec.* **2023**, *9*, 1–13. [CrossRef]
26. Witten, P.E.; Hall, B.K. Differentiation and growth of kype skeletal tissues in anadromous male Atlantic salmon (*Salmo salar*). *Int. J. Dev. Biol.* **2002**, *46*, 719–730. Available online: https://oceanrep.geomar.de/id/eprint/7095/ (accessed on 20 March 2024). [PubMed]
27. Fonseca, V.G.; Joana Rosa, J.; Laizé, V.; Gavaia, P.J.; Cancela, M.L. Identification of a new cartilage-specific S100-like protein up-regulated during endo/perichondral mineralization in gilthead seabream. *Gen. Exp. Patt.* **2011**, *11*, 448–455. [CrossRef] [PubMed]
28. Weigele, J.; Franz-Odendaal, T.A. Functional bone histology of zebrafish reveals two types of endochondral ossification, different types of osteoblast clusters and a new bone type. *J. Anat.* **2016**, *229*, 92–103. [CrossRef] [PubMed]
29. Masiero, C.; Aresi, C.; Forlino, A.; Tonelli, F. Zebrafish models for skeletal and extraskeletal osteogenesis imperfecta features: Unveiling pathophysiology and paving the way for drug discovery. *Cal. Tiss. Int.* **2024**, *115*, 931–959. [CrossRef]

30. Witten, P.E.; Hall, B.K. Seasonal changes in the lower jaw skeleton in male Atlantic salmon (*Salmo salar* L.): Remodeling and regression of the kype after spawning. *J. Anat.* **2003**, *203*, 435–450. [CrossRef]
31. Dean, M.N.; Ekstrom, L.; Monsonego-Ornan, E.; Ballantyne, J.; Witten, P.E.; Riley, C.; Habraken, W.; Omelon, S. Mineral homeostasis and regulation of mineralization processes in the skeletons of sharks, rays and relatives (Elasmobranchii). *Semin. Cell Dev. Biol.* **2015**, *46*, 51–67. [CrossRef]
32. Mhalhel, K.; Levanti, M.; Abbate, F.; Laurà, R.; Guerrera, M.C.; Aragona, M.; Porcino, C.; Pansera, L.; Sicari, M.; Cometa, M.; et al. Skeletal morphogenesis and anomalies in Gilthead Seabream: A comprehensive review. *Int. J. Mol. Sci.* **2023**, *24*, 16030. [CrossRef]
33. Le Pabic, P.; Dranow, D.B.; Hoyle, D.J.; Schilling, T.F. Zebrafish endochondral growth zones as they relate to human bone size, shape and disease. *Front. Endocrinol.* **2022**, *13*, 1060187. [CrossRef]
34. Gai, Z.; Zhu, M. The origin of the vertebrate jaw: Intersection between developmental biology-based model and fossil evidence. *Chin. Sci. Bull.* **2012**, *57*, 3819–3828. [CrossRef]
35. Zhao, Q.; Eberspaecher, H.; Lefebvre, V.; De Crombrugghe, B. Parallel expression of Sox9 and Col2a1 in cells undergoing chondrogenesis. *Dev. Dyn.* **1997**, *209*, 377–386. [CrossRef]
36. Ng, L.J.; Wheatley, S.; Muscat, G.E.; Conway-Campbell, J.; Bowles, J.; Wright, E.; Bell, D.M.; Tam, P.P.; Cheah, K.S.; Koopman, P. SOX9 binds DNA, activates transcription, and coexpresses with type II collagen during chondrogenesis in the mouse. *Dev. Biol.* **1997**, *183*, 108–121. [CrossRef]
37. Marconi, A.; Hancock-Ronemus, A.; Gillis, J.A. Adult chondrogenesis and spontaneous cartilage repair in the skate, *Leucoraja erinacea*. *Elife* **2020**, *12*, e53414. [CrossRef]
38. Dale, R.M.; Topczewski, J. Identification of an evolutionarily conserved regulatory element of the zebrafish col2a1a gene. *Dev. Biol.* **2011**, *357*, 518–531. [CrossRef] [PubMed]
39. Enault, S.; Muñoz, D.N.; Silva, W.T.A.F.; Borday-Birraux, V.; Bonade, M.; Oulion, S.; Ventéo, S.; Marcellini, S.; Debiais-Thibaud, M. Molecular footprinting of skeletal tissues in the catshark *Scyliorhinus canicula* and the clawed frog *Xenopus tropicalis* identifies conserved and derived features of vertebrate calcification. *Front. Genet.* **2015**, *6*, 283. [CrossRef]
40. Donato, R. Intracellular and extracellular roles of S100 proteins. *Microsc. Res. Technol.* **2003**, *60*, 540–551. [CrossRef] [PubMed]
41. Kraemer, A.M.; Saraiva, L.R.; Korsching, S.I. Structural and functional diversification in the teleost S100 family of calcium-binding proteins. *BMC Evol. Biol.* **2008**, *8*, 48. [CrossRef] [PubMed]
42. Courties, A.; Do, A.; Leite, S.; Legris, M.; Sudre, L.; Pigenet, A.; Petit, J.; Nourissat, G.; Cambon-Binder, A.; Maskos, U.; et al. The role of the non-neuronal cholinergic system in inflammation and degradation processes in osteoarthritis. *Arth. Rheum.* **2020**, *72*, 2072–2082. [CrossRef]
43. Ohsawa, K.; Imai, Y.; Kanazawa, H.; Sasaki, Y.; Kohsaka, S. Involvement of Iba1 in membrane ruffling and phagocytosis of macrophages/microglia. *J. Cell Sci.* **2000**, *113*, 3073–3084. [CrossRef]
44. Huang, Y.; Wang, X.; Zhou, D.; Zhou, W.; Dai, F.; Lin, H. Macrophages in heterotopic ossification: From mechanisms to therapy. *Npj Regen. Med.* **2021**, *6*, 70. [CrossRef]
45. Hu, Y.; Huang, J.; Chen, C.; Wang, Y.; Hao, Z.; Chen, T.; Wang, J.; Li, J. Strategies of macrophages to maintain bone homeostasis and promote bone repair: A narrative review. *J. Funct. Biomater.* **2022**, *14*, 18. [CrossRef] [PubMed]
46. Khajavi, M.; Hajimoradloo, A.; Zandi, M.; Pezeshki-Modaress, M.; Bonakdar, S.; Zamani, A. Fish cartilage: A promising source of biomaterial for biological scaffold fabrication in cartilage tissue engineering. *J. Biomed. Mater. Res.* **2021**, *109*, 1737–1750. [CrossRef] [PubMed]
47. Zhao, T.; Zhou, Y.; Mao, G.; Zou, Y.; Zhao, J.; Bai, S.; Yang, L.; Wu, X. Extraction, purification and characterization of chondroitin sulfate in Chinese sturgeon cartilage. *J. Sci. Food Agric.* **2013**, *93*, 1633–1640. [CrossRef]
48. Kan, S.; Duan, M.; Liu, Y.; Wang, C.; Xie, J. Role of mitochondria in physiology of chondrocytes and diseases of osteoarthritis and rheumatoid arthritis. *Cartilage* **2021**, *13*, 1102S–1121S. [CrossRef] [PubMed]
49. Gvaramia, D.; Kern, J.; Jakob, Y.; Zenobi-Wong, M.; Rotter, N. Regenerative potential of perichondrium: A tissue engineering perspective. *Tissue Eng. Part B. Rev.* **2022**, *28*, 531–541. [CrossRef]
50. Root, Z.D.; Gould, C.; Brewer, M.; Jandzik, D.; Medeiros, D.M. Comparative approaches in vertebrate cartilage histogenesis and regulation: Insights from Lampreys and Hagfishes. *Diversity* **2021**, *13*, 435. [CrossRef]
51. Klein, M.; Csöbönyeiová, M.; Danišovič, Ľ.; Lapides, L.; Varga, I. Telocytes in the female reproductive system: Up-to-Date knowledge, challenges and possible clinical applications. *Life* **2022**, *12*, 267. [CrossRef]
52. Verdile, N.; Pasquariello, R.; Cardinaletti, G.; Tibaldi, E.; Brevini, T.A.L.; Gandolfi, F. Telocytes: Active players in the rainbow trout (*Oncorhynchus mykiss*) intestinal stem-cell niche. *Animals* **2022**, *12*, 74. [CrossRef]
53. Mokhtar, D.M. Functional morphology of cardiac stomach of Nile catfish (*Clarias gariepinus*): Histological, scanning, and ultrastructural studies. *Microsc. Res. Technol.* **2022**, *85*, 1845–1855. [CrossRef]

54. Zaccone, G.; Mokhtar, D.M.; Alesci, A.; Capillo, G.; Albano, M.; Hussein, M.T.; Aragona, M.; Germanà, A.; Lauriano, E.R.; Sayed, R.K.A. From proliferation to protection: Immunohistochemical profiling of cardiomyocytes and immune cells in Molly Fish hearts. *Fishes* **2024**, *9*, 283. [CrossRef]
55. Gandahi, N.S.; Ding, B.; Shi, Y.; Bai, X.; Gandahi, J.A.; Vistro, W.A.; Chen, Q.; Yang, P. Identification of telocytes in the pancreas of Turtles—A role in cellular communication. *Int. J. Mol. Sci.* **2020**, *21*, 2057. [CrossRef] [PubMed]
56. Condrat, C.E.; Barbu, M.G.; Thompson, D.C.; Dănilă, C.A.; Boboc, A.E.; Suciu, N.; Crețoiu, D.; Voinea, S.C. Roles and distribution of telocytes in tissue organization in health and disease. In *Tissue Barriers in Disease, Injury and Regeneration*; Gorbunov, N.V., Ed.; Elsevier Ltd.: Amsterdam, The Netherlands, 2021; pp. 1–41. [CrossRef]